JGR Biogeosciences

RESEARCH ARTICLE
10.1029/2023JG007814

Net Methane Production Predicted by Patch Characteristics in a Freshwater Wetland

Sean J. Sharp[1], Christine E. Maietta[2], Graham A. Stewart[1], Aileen K. Taylor[1], Michael R. Williams[1], and Margaret A. Palmer[1,2]

[1]Department of Entomology, University of Maryland, College Park, MD, USA, [2]National Socio-Environmental Synthesis Center, Annapolis, MD, USA

Key Points:

- Herbaceous plant patches present a unit of measure that can integrate multiples scales controlling wetland methane dynamics
- Methane dynamics in the soil are linked to plant-mediated rhizosphere oxygenation, litter quality, and DOC composition
- Grass and sedge functional types seem to modulate methane via different mechanisms, highlighting the importance of using functional type

Supporting Information:

Supporting Information may be found in the online version of this article.

Correspondence to:

S. J. Sharp,
seanjsharp@gmail.com

Citation:

Sharp, S. J., Maietta, C. E., Stewart, G. A., Taylor, A. K., Williams, M. R., & Palmer, M. A. (2024). Net methane production predicted by patch characteristics in a freshwater wetland. *Journal of Geophysical Research: Biogeosciences*, *129*, e2023JG007814. https://doi.org/10.1029/2023JG007814

Received 21 SEP 2023
Accepted 5 DEC 2023

Author Contributions:

Conceptualization: Sean J. Sharp, Christine E. Maietta, Graham A. Stewart, Aileen K. Taylor, Michael R. Williams, Margaret A. Palmer
Data curation: Sean J. Sharp, Christine E. Maietta
Formal analysis: Sean J. Sharp, Christine E. Maietta
Funding acquisition: Margaret A. Palmer

Abstract Methane (CH_4) dynamics in wetlands are spatially variable and difficult to estimate at ecosystem scales. Patches with different plant functional types (PFT) represent discrete units within wetlands that may help characterize patterns in CH_4 variability. We investigate dissolved porewater CH_4 concentrations, a representation of net CH_4 production and potential source of atmospheric flux, in five wetland patches characterized by a dominant PFT or lack of plants. Using soil, porewater, and plant variables we hypothesized to influence CH_4, we used three modeling approaches—Classification and regression tree, AIC model selection, and Structural Equation Modeling—to identify direct and indirect influences on porewater CH_4 dynamics. Across all three models, dissolved porewater CO_2 concentration was the dominant driver of CH_4 concentrations, partly through the influence of PFT patches. Plants in each patch type likely had variable influence on CH_4 via root exudates (a substrate for methanogens), capacity to transport gas (both O_2 from and CH_4 to the atmosphere), and plant litter quality which impacted soil respiration and production of CO_2 in the porewater. We attribute the importance of CO_2 to the dominant methanogenic pathway we identified, which uses CO_2 as a terminal electron acceptor. We propose a mechanistic relationship between PFT patches and porewater CH_4 dynamics which, when combined with sources of CH_4 loss including methanotrophy, oxidation, or plant-mediated transport, can provide patch-scale estimates of CH_4 flux. Combining these estimates with the distribution of PFTs can improve ecosystem CH_4 flux estimates in heterogenous wetlands and improve global CH_4 budgets.

Plain Language Summary Methane is a potent greenhouse gas and understanding what controls methane production from microbes to plant communities can improve our estimates of wetland fluxes and global methane budgets. We propose characterizing methane dynamics in herbaceous wetlands at the scale of plant patches as patches integrate multiple local properties, are generally discrete, and relatively easy to map and measure. To characterize common wetland patch types, we investigate patterns of dissolved methane, soil biogeochemistry, and plant properties in 4 vegetated (submerged vegetation, forb, grass, and sedge) and 1 unvegetated wetland patch types in a temperate, freshwater, herbaceous wetland. We found that methane production differs significantly across patches and is largely correlated with each plant's capacity to transport gas to and from the soil, the quality of plant litter, and the properties of dissolved organic carbon in each patch. This work improves our understanding of how patches uniquely influence methane and by mapping the distribution of these patches we can improve our estimates of wetland methane fluxes.

1. Introduction

Linking disparate spatial and temporal scales of biogeochemical cycles and ecosystem function is the next frontier of environmental science (Körner, 2014; National Research Council, 2001). Microbially mediated methane (CH_4) cycling, which integrates processes from microbes to ecosystems, presents an avenue to explore this frontier. Identifying appropriate scales to measure CH_4 cycling that both capture drivers of microbial production and represent ecosystem heterogeneity is critical to understanding ecosystem atmospheric fluxes. At the plant community level, the variability of important CH_4 drivers including anoxia and organic matter (OM) is constrained by stabilizing feedbacks between plants and soil and the adaptation of plant species to certain conditions (Cottenie, 2005; Donohue et al., 2013; Metcalfe et al., 2011). This reinforcing stability can lead to plant communities with discrete borders and a predictable range of local conditions (Bertness & Leonard, 1997; Wilson & Agnew, 1992). Thus, understanding what drives CH_4 production, consumption, and transport at plant community or local patch scales

Investigation: Sean J. Sharp, Christine E. Maietta, Graham A. Stewart, Aileen K. Taylor, Michael R. Williams, Margaret A. Palmer
Methodology: Sean J. Sharp, Christine E. Maietta, Graham A. Stewart, Aileen K. Taylor, Michael R. Williams, Margaret A. Palmer
Project Administration: Sean J. Sharp, Margaret A. Palmer
Resources: Sean J. Sharp, Margaret A. Palmer
Supervision: Sean J. Sharp, Margaret A. Palmer
Validation: Sean J. Sharp
Visualization: Sean J. Sharp, Christine E. Maietta, Michael R. Williams, Margaret A. Palmer
Writing – original draft: Sean J. Sharp
Writing – review & editing: Sean J. Sharp, Christine E. Maietta, Graham A. Stewart, Aileen K. Taylor, Michael R. Williams, Margaret A. Palmer

could help us build bottom-up models that integrate heterogeneous wetlands to better manage or anticipate CH_4 emissions in the future.

As microbially mediated CH_4 production occurs almost exclusively under anoxic conditions (Reddy & DeLaune, 2008), wetland ecosystems characterized by anoxia are hotspots for CH_4 production contributing up to 31% to global CH_4 budgets (Saunois et al., 2020). Methane cycling in wetlands is influenced by many environmental drivers, each operating at different temporal and spatial scales. At small scales and faster rates, biogeochemical and microbial dynamics dominate. OM is also necessary as a substrate for methanogenesis, and the amount and composition of OM affect rates of CH_4 production (Berberich et al., 2020). Variables that control anoxia (e.g., hydrology) and OM (e.g., vegetation) within these ecosystems are thus important drivers of CH_4 production. Other controls on CH_4 production range from simple thermodynamic relationships (e.g., temperature; Inglett et al., 2012) to microbial community composition and structure (e.g., resource competition and CH_4 consumption; Bridgham et al., 2013) and ecosystem dynamics (e.g., exogeneous inputs and influences of other biota; Silvey et al., 2019).

Plants are also known to influence soil CH_4 cycling and contribute variability to ecosystem-scale estimates of CH_4 flux (Joabsson et al., 1999). Plant physiology (e.g., belowground and aboveground tissue chemistry, litter quality, and canopy height) and phenology (e.g., annual productivity, timing of spring emergence, and fall senescence) play critical roles in modulating ecosystem properties and soil CH_4 dynamics (Moor et al., 2017; Mueller et al., 2020). Plant rooting zones are biogeochemically active and spatially heterogeneous areas. Roots simultaneously exude simple organic compounds that fuel CH_4 production and supply oxygen that supports CH_4 oxidation and consumption (Waldo et al., 2019). Plant traits like rooting depth and specific root length determine the contact area between roots and the surrounding soil, the volume of rhizosphere, and the potential for both transporting CH_4 from, and oxygen to the soil (Butterbach-Bahl et al., 1997; Gerard & Chanton, 1993; Von Fischer et al., 2010). Aboveground, canopy height can influence CH_4 through the amount of leaf tissue above the water surface and the density of gas-conducting stomata (Morrissey et al., 1993). Gas transport rates are also controlled by the density of porous aerenchyma tissue which acts as a plant's gas conduit (Butterbach-Bahl et al., 1997). Further, plants provide OM to soil for microbial oxidation through litter deposition and organic root exudates (Valentine et al., 1994; Waldo et al., 2019). Though vegetation is known to influence CH_4 flux in wetlands, few have linked vegetation to dynamics in dissolved CH_4 in porewater or CH_4 production in the soil (but see Bansal et al., 2020; Noyce & Megonigal, 2021).

Herbaceous wetlands, characterized by a mosaic of discrete plant communities or patches, can exhibit high variability in soil anoxia and OM. Assigning single CH_4 flux values or parameters to whole wetlands fails to capture important spatial heterogeneity, resulting in estimates of ecosystem CH_4 fluxes that can differ by more than 50% (Schrier-Uijl et al., 2010). The distribution of patches often results from species sorting through environmental filters, expansion via clonal or vegetative reproduction, and reinforcing feedbacks (Lozada-Gobilard et al., 2019; Weiher & Keddy, 1995). Incorporating plant patches into flux estimates should account for the heterogeneity of both plants and the environmental conditions plant communities naturally integrate, like hydrology and anoxia. By leveraging this organization, we can attempt to identify common patch properties known to influence CH_4 cycling, better model CH_4 production at community scales, and attempt to control CH_4 through vegetation management.

We sought to identify patterns in CH_4 production by investigating dissolved CH_4 concentrations in soil porewater—where CH_4 is primarily produced in our system—within discrete patches defined by dominant plant functional types (PFTs; Woodward & Cramer, 1996). Using measurements of biotic and abiotic conditions, we aim to describe wetland plant communities as suites of co-occurring CH_4 drivers. Our goal was to determine if there were differences in these conditions among patch types and if so, which conditions best predict CH_4 dynamics. Specifically, we hypothesized that (a) biomass and physiology (e.g., stem height) of PFTs would correlate with porewater DOC, (b) DOC quality (e.g., aromaticity) would modulate CH_4 production and reflect inputs of each patch PFT, and (c) the conditions that control porewater CH_4 would change over time with seasonal shifts in the soil environment and the specific phenology of each PFT.

Our findings demonstrate strong interpatch variability and identify key mechanisms controlling CH_4 production that plant patches integrate. Since discrete plant communities can be mapped with ground surveys and remote sensing, using their combined contribution to CH_4 cycling has the potential to refine estimates of ecosystem CH_4 flux.

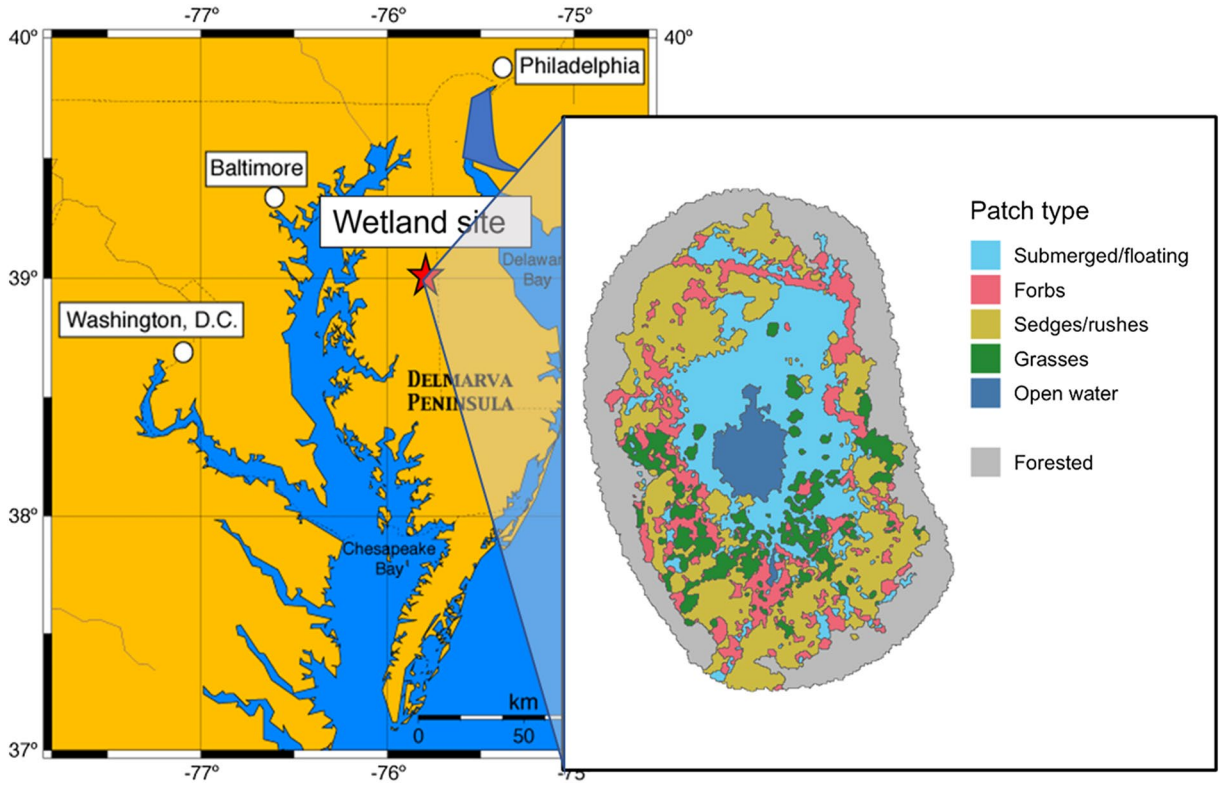

Figure 1. Location of study wetland and inset of distribution of patches representing four Plant Functional Types and on unvegetated open water in the wetland.

2. Materials and Methods

2.1. Study Site

For this study we investigated soil CH_4 production within patches of an isolated, herbaceous 1.33 ha wetland on the Delmarva Peninsula, Maryland, USA (Figure 1; 39.054 N 75.753 W). The wetland is nested within a conservation area, surrounded by forest and agricultural land. Based on hydrology and water chemistry data, including conductivity and nutrient concentrations, farms have little influence or input into our study wetland (i.e., the study wetland had low nutrient concentrations and rarely has overland hydrological connections to water channels) allowing us to characterize nutrient and OM inputs as primarily autochthonous. Our study site is equipped with an eddy-covariance flux tower allowing us to monitor a suite of environmental variables, including air temperature, precipitation, and ecosystem greenhouse gas (CO_2 and CH_4) fluxes using Licor LI-7500 and LI-7700 open patch sensors. Although the 10-year average annual rainfall for this area is approximately 1,100 mm y^{-1}, our study in 2021 was wet with an annual total of 1,555 mm resulting in standing water throughout much of the study (Figure S1 in Supporting Information S1).

2.2. Vegetation Patches

Within the study site, we chose five patches anticipated to have distinct influences on soil biogeochemistry and CH_4 dynamics (Figure 2b). Of these patch types, four were colonized by different plant functional types (PFT): sedges (*Carex striata*, SEG), grasses (*Panicum hemitomon*, GRA), forbs (emergent *Persicaria hydropiperoides*, FORB), and a mix of submerged aquatic vegetation including *Proserpinica* spp. and *Juncus repens* (SAV). The fifth patch represented unvegetated open water (OPW) and remained uncolonized throughout the year. Each of our PFTs are common and widespread across eastern North America (https://plants.usda.gov, see Figure 2c, Table 1, and Boutin & Keddy, 1993 for details about each PFT). One PVC well outfitted with a pressure transducer (HOBO U20-001-04) was installed in each patch type, referenced to the soil surface and corrected for barometric pressure to monitor water level throughout the study. Within each of the patch types and several months before sampling, we established 3 replicate plots surrounded by a >2 m buffer of the dominant vegetation for

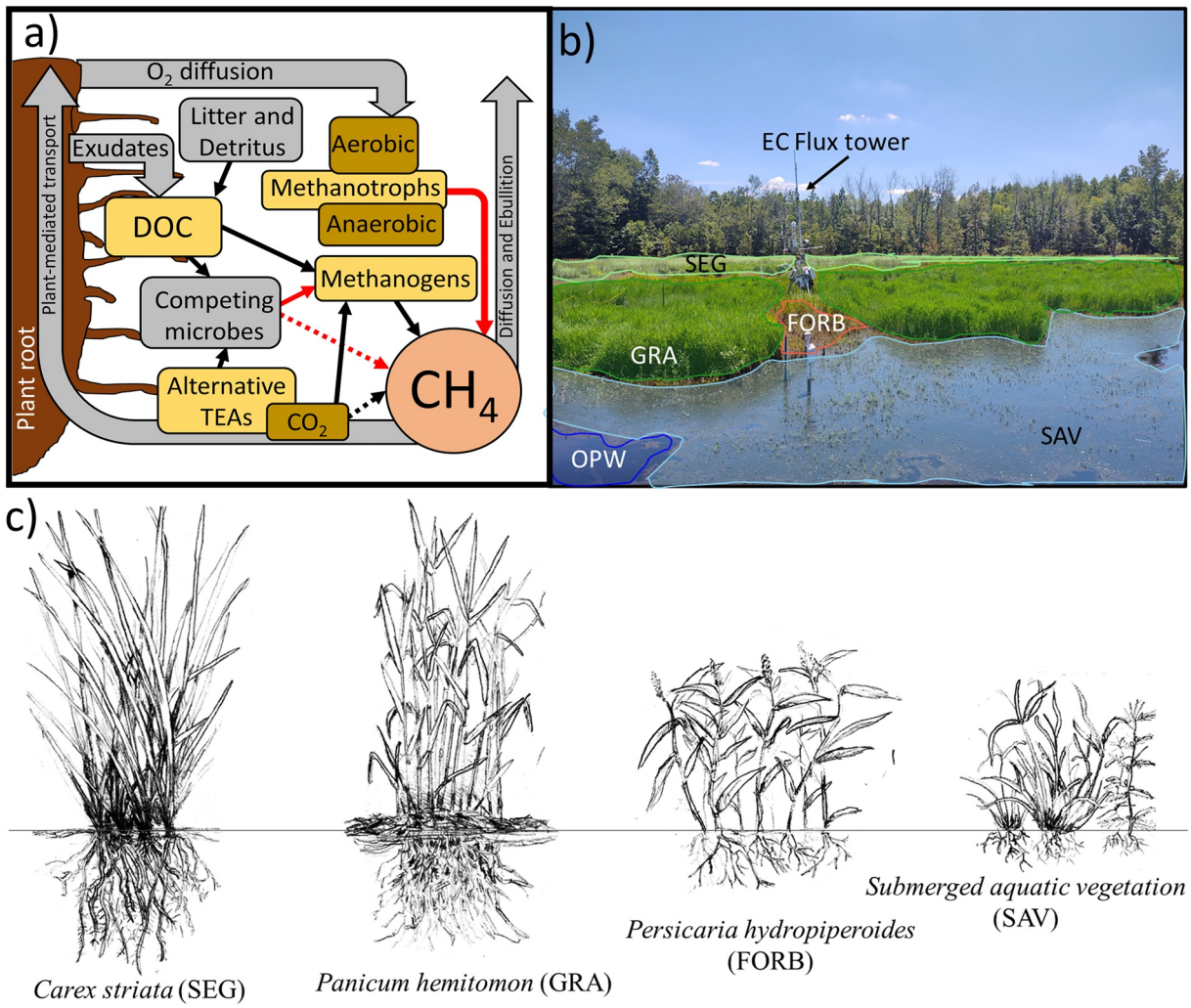

Figure 2. Soil CH_4 diagram (a) showing predicted drivers and pathways of porewater CH_4 (orange circle) imposed on 4 vegetated and 1 unvegetated wetland patch types (b) in our study wetland near Goldsboro, MD, USA. In (a), red arrows indicate negative effects, black arrows positive effects, and dashed arrows indicate indirect effects. Plant morphology sketch (c) reflects aboveground biomass and rooting density and depth (not to scale). Gray boxes and arrows in (a) indicate known direct and indirect influences on CH_4 that we did not measure in this study. DOC = Dissolved Organic Carbon, TEAs = terminal electron acceptors, SEG = sedges, GRA = grasses, FORB = forbs, SAV = submerged aquatic vegetation, OPW = open water.

instrumentation and monitoring (5 patch types ×x 3 replicate plots = 15 total plots). Although we only investigate a single species from each PFT, we attempt to overcome this shortcoming through high sampling resolution (n = 75 porewater samples per patch over 5 campaigns) and robust analysis intended to infer mechanistic relationships between PFTs and porewater CH_4.

2.3. Porewater Sampling and Laboratory Analyses

In each of the 3 replicate plots per patch type we installed Rhizon porous porewater samplers (Rhizosphere Research Products) with 0.15 μm pore size several months before our first sampling (n = 75). We dug soil pits >40 cm deep and inserted Rhizons horizontally into the side wall at 10 cm depth increments starting just under the litter layer (designated "0 cm") to 40 cm deep (5 total Rhizon depths). We then ran 100 cm of gas impermeable tubing from the Rhizon to a sampling port at the surface fitted with a stopcock to prevent gas exchange with the surrounding soil. Two months before our first sampling campaign, we installed an elevated boardwalk to minimize disturbance to surface water and soils during sampling. We chose 5 sampling campaign dates to capture seasonal shifts in organic matter inputs, hydrology, plant phenology, and weather: 23 June, 25 July, 14 September, 1 November 2021, and 11 April 2022.

Table 1
Patch Characteristics of 4 Plant Functional Types and Unvegetated Open Water

	Sedges	Grasses	Forbs	Submerged aquatic vegetation	Open water
ID	SEG	GRA	FORB	SAV	OPW
Dominant species	*Carex striata*	*Panicum hemitomon*	*Persicaria hydropiperoides*	*Proserpinica* spp. *Juncus repens* *P hydropiperoides* (submerged)	--
Photosynthetic pathway	C_3	C_3	C_3	$C_{3/4}$	--
Peak aboveground biomass (g/m^2)	80.1 ± 10.2	141 ± 10.8	127 ± 16.4	34.9 ± 6.9	0.00
Root biomass 0–10 cm (g/m^2)	55.4 ± 4	25.7 ± 12	2.9 ± 1	1.8 ± 0.0	0.00
Root biomass >10 cm (g/m^2)	36.9 ± 12	37.0 ± 28	1.75 ± 0.0	8.6 ± 0.0	1.5 ± 0.0
Indicator	OBL	OBL	OBL	OBL	--
Growth type	Clumping	Lateral spreader	Seeder	Seeder	--
C:N ratio	58.48[a]	90.4[b]	9.46–16.47[c]	10.78[c]	--
Aerenchyma tissue	Y	Y	Y	Y	--
Water depth (m)	0.23 ± 0.06	0.29 ± 0.06	0.39 ± 0.07	0.46 ± 0.06	0.49 ± 0.06

Note. Numeric values in mean ± S.E.
[a]Burrow and Maerz (2021). [b]Moran et al. (1989). [c]Ren et al. (2022).

We sampled porewater by attaching 60 ml Luer-Lock syringes to each Rhizon port ($n = 75$) and extending plungers to create a vacuum in the syringe barrel. Syringes were left undisturbed for up to 2 hr until at least 35 ml of porewater was extracted. An aliquot of porewater was used to measure Fe^{2+}, an indicator of soil redox conditions, using the ferrozine method (see supplement for methods). Dissolved gases were extracted from porewater samples within 24 hr using the headspace equilibrium method (Kling et al., 1991). Equilibrated syringe headspace was then transferred into evacuated 12 ml vials for laboratory analysis of CH_4 and CO_2 concentrations. Remaining porewater samples were then stored at 4°C and later analyzed for DOC concentrations, DOC optical properties ($SUVA_{254}$, and Spectral Slope Ratio, S_R), and alternative terminal electron acceptors $Fe^{2+}Fe^{3+}$, NH_4^+/NO_3^-, and SO_4^{2-} (see supplement for methods). [SO_4^{2-}], [NH_4^+], and [NO_3^-] concentrations were only measured during the June campaign.

2.4. Plant Biomass

To determine if aboveground plant biomass is related to CH_4 porewater concentrations, we counted live plant stems and measured the height of the 5 tallest stems within 0.5 × 0.5 m quadrats adjacent to Rhizon sampling ports in SEG, GRA, and FORB plots. We also estimated percent cover of live and dead vegetation and measured water and soil temperatures at each Rhizon depth (0–40 cm). For SAV plots, we could not count or measure heights of stems and thus used percent live cover and water depth. Plant metrics were used to estimate aboveground biomass at each sampling campaign (Equation 1 below). During peak plant growth (July), we harvested plant tissue above the soil surface from 3–0.5 × 0.5 m quadrats in each vegetated patch type, counted and measured stem heights, dried at 65°C for 48 hr, and weighed for dry biomass. To estimate aboveground biomass nondestructively for each sampling campaign we parameterized a linear allometric equation (Equation 1) for SEG ($R^2 = 0.98$), GRA ($R^2 = 0.95$), and FORB ($R^2 = 0.68$) patch types by fitting dried biomass to stem count and canopy height values

$$\beta_1 * \text{Stem Count} + \beta_2 * \text{Canopy Height} + \alpha = \text{Aboveground Biomass}\left(\text{dry weight g m}^{-2}\right) \quad (1)$$

Duplicate soil cores to 40 cm depth were collected from each plot ($n = 30$ cores) at the end of the study (Summer 2022) using 4 cm diameter stainless steel, beveled-edge corers. One core was used to determine root biomass; cores were divided into 4 depth increments corresponding generally to horizons, 0–10, 11–20, 21–30, and 31–40 cm and wet sieved through 2 mm sieves, then the roots picked out by hand. Roots from deeper soil horizons (>11 cm) were aggregated due to diminishing biomass within this soil range. Sorted roots were dried for 48 hr at 65°C and weighed. Belowground biomass (g/m^3) was calculated by dividing dry root weight by sample depth × core surface area.

2.5. Soil Properties

To measure soil organic carbon (SOC) and particle size distribution, soil from the second core was again divided into 10 cm depth increments (0–10, 11–20, 21–30, and 31–40), air dried for at least 48 hr, ground, and passed through a 2 mm mesh sieve. Subsamples of 50 g from each depth increment of 3 patches (GRA, SAV, and OPW, $n = 12$) were sent to Brookside Laboratories (Bremen, OH, USA) for particle size analysis. For estimating SOC, 5 g subsamples of each core section ($n = 60$) were combusted at 550°C for 2 hours and weighed to calculate Loss on Ignition (LOI). Of the 60 core sections, a subset of 20 representing all patches and a span of depth increments was selected to measure SOC using an elemental CHN analyzer (LECO CHN-2000 Analyzer). These values were then regressed with their matching LOI values ($R^2 = 0.84$) to estimate SOC from all soil core sections (Figure S2 in Supporting Information S1; Craft et al., 1991).

2.6. Soil Microbial Community Analysis

To characterize the microbial community, duplicate soil cores were collected from each plot in April and July 2021 using a 30.5 cm soil probe. Each core was visually divided into three master horizons, O ("top"), A ("middle"), and B ("bottom") to represent varying microbial activity. To compare microbial communities from each horizon to porewater characteristics measured from Rhizons and our other cores, we matched SOC content of O, A, and B horizons to that of each 10 cm subdivision and binned those values (porewater and soil) into one of the three horizons. Duplicate sections were placed into a sterile sampling bag, where all excess air was removed prior to sealing, and gently homogenized into a single representative sample. Soil samples were immediately placed in a cooler containing dry ice and then transferred to a −80°C freezer upon returning from the field. A total of 90 soil samples were collected across the spring and summer field campaigns (5 patches × 3 replicate plots × 3 horizons × 2 campaigns). Due to budget constraints, we collected samples from 3 of 5 patches that we anticipated would have significant differences, GRA, FORB, and OPW, representing emergent graminoid vegetation, a forb, and unvegetated control, respectively. In our previous research, we found DNA yields from lower clay-rich horizons (i.e., B horizons) were not sufficient for sequencing; therefore, we proceeded with only the top two horizons (O and A). A total of 36 samples were sent on dry ice for DNA/RNA extraction and DNA sequencing (Microbiome Service Laboratory, Baltimore, Maryland). We then calculated the relative abundance by dividing the total number of identified microbial OTUs present in each sample by the total number of OTUs observed in each sample × 100. We then binned OTUs into methanogens, anaerobic methanotrophs, and aerobic methanotrophs.

2.7. Statistical Analysis

All statistical analyses were conducted in R v 4.2.2 (R Core Team, 2019). To determine the relationship between potential drivers of porewater CH_4, we employed a suite of analyses that account for both categorial and continuous variables and are capable of handling missing data or hierarchical data structure (e.g., depth nested within patch). We first z-transformed all data to allow comparison of standardized effect sizes. Porewater CH_4, aboveground biomass, and relative abundance of methanogens were log-transformed to meet assumptions of normality.

2.7.1. Differences Across Vegetation Patches

To identify potential differences among patch types in porewater terminal electron acceptors and dissolved CH_4, as well as CH_4 cycling microbes, we used a repeated measure Two-way Analysis of Variance (ANOVA, Patch × Horizon) with plot assigned as a random effect (these plots were measured repeatedly at each campaign).

To explore correlations between patch characteristics and relative abundance (RA) of CH_4 cycling microbes, we used linear mixed-effects models to compare RA with soil [CH_4], [CO_2], [DOC], SUVA, S_r, [NH_4^+], [NO_3^-], [SO_4^{2-}], and [SOC] and plant (biomass and canopy height) variables during the time of microbial sampling (April–July 2021). We only compared CH_4 producers (methanogens), and CH_4 consumers (aerobic and anaerobic methanotrophs) that would have direct effects on CH_4 cycling. As we found no significant difference in microbial abundance over time, we did not consider campaign date as a predictor variable but included it and plot as random effects.

2.7.2. Predictors of Porewater Methane

To explore potential drivers of CH_4 concentrations, we completed two analyses. First, we built a classification and regression tree that split predictor variables based on their correlation with porewater CH_4. This was done

using the ANOVA method of recursive partitioning, which iteratively splits the data into partitions that minimize the sum of squared deviations from the response variable mean (CH_4) in each of the two parts. We chose 0.08 as the complexity parameter, a relatively conservative value that defines the minimum improvement to the R^2 value necessary to create a split in the tree, and a 10-fold cross-validation using the rpart R package (Therneau & Atkinson, 2017). We used patch, canopy height, aboveground biomass, $SUVA_{254}$, S_R, [DOC], SOC, soil temperature, Fe^{2+}, dissolved [CO_2], and Julian date as predictor variables for our regression tree. Second, to determine the combination of variables that best predicted [CH_4], we created generalized linear mixed-effects models (GLMM) of all variable combinations using lme4 R package and then ranked best model fit by Akaike Information Criterion (AIC) values (Bates et al., 2015). For this study, we only considered linear relationships.

2.7.3. Relative Strength of Predictors

To quantify the direct and indirect effects of patch characteristics on porewater CH_4, we constructed structural equation models using the R package piecewiseSEM, a form of confirmatory path analysis (Lefcheck, 2016). As piecewiseSEM requires relatively large data sets we were limited to using complete data sets collected over the campaigns and excluded variables measured infrequently ([NH_4^+], [NO_3^-], [SO_4^{2-}], SOC, belowground biomass, and microbial abundance). We first constructed an a priori causal diagram using important predictors found in our previous models (Figure 2a). To account for categorical variables in the SEM, standard estimates and pairwise contrasts of patches were calculated using the emmeans R package (Lenth, 2023). To identify potential multicollinearity among variables before constructing SEMs, we calculated Variable Inflation Factors (VIFs). After initial pathways were identified and input into the SEM, we used tests of directed separation to find missing pathways (deemed important at $P < 0.05$) or removed pathways that had little explanatory power (high P-value and/or low R^2) and whose removal improved overall model fit. Finally, we evaluated global goodness-of-fit using Fisher's C value with a higher P-value indicating a better fit (i.e., closer approximation of observed and modeled data). We used plot as a random effect in LMR and SEM to account for repeated measures in plots over time.

3. Results

We found significant differences in porewater variables including CH_4 concentrations and those hypothesized as predictors of [CH_4] between patches, across soil depth, and over time.

3.1. Porewater

Among patches, OPW and SAV generally had the highest average porewater [CH_4] and highest $SUVA_{254}$—an indication of higher molecular aromaticity (Figures 3 and 4). OPW also had relatively high [DOC] and low porewater CO_2 concentrations ([CO_2]; Figure 5; Figure S3 in Supporting Information S1). Emergent patches SEG and GRA had relatively low [CH_4] while SEG and FORB had low $SUVA_{254}$. Like OPW, GRA had relatively low porewater [CO_2], while FORB generally had the most [CO_2].

[CH_4] was always highest in the O horizon (0–20 cm) and lowest in the A and B horizons (21–40 cm) regardless of patch (Figure 3). However, $SUVA_{254}$, an optical property of DOC whose higher values indicates plant-like, aromatic DOC and lower values more microbial-like DOC, interacted between horizons and patches and varied across campaigns (Figure 4). SUVA was consistently highest in OPW patches. Yet in November, OPW SUVA was highest in the O horizon, but lowest while GRA waws highest in the B horizon There was no interaction between depth and patch in June and July.

In SEG, FORB, and SAV patches, [CO_2] and [DOC] strongly interacted with campaign. [CO_2] was highest during summer campaigns (June-September) in FORB patches and highest in SEG in April and November (Figure 5). Compared to other patches, SEG had relatively low [DOC] in April and June yet relatively high in July, September, and November (Figure S3 in Supporting Information S1). SAV [DOC] patterns were the opposite (i.e., higher in April and June and lower the rest of the year).

SO_4^{2-} concentrations ([SO_4^{2-}]) represent both the potential for energetically favorable sulfate-reducing microbes to outcompete methanogens and the redox condition of soil, with high [SO_4^{2-}] indicating frequent oxygenation of the soil (Wiessner et al., 2010). [SO_4^{2-}] was more than three times higher in FORB than GRA and SAV and higher at depth (B horizon, Table S1 in Supporting Information S1). Other porewater variables did not exhibit strong patterns and were unlikely to influence CH_4 dynamics differently across patches.

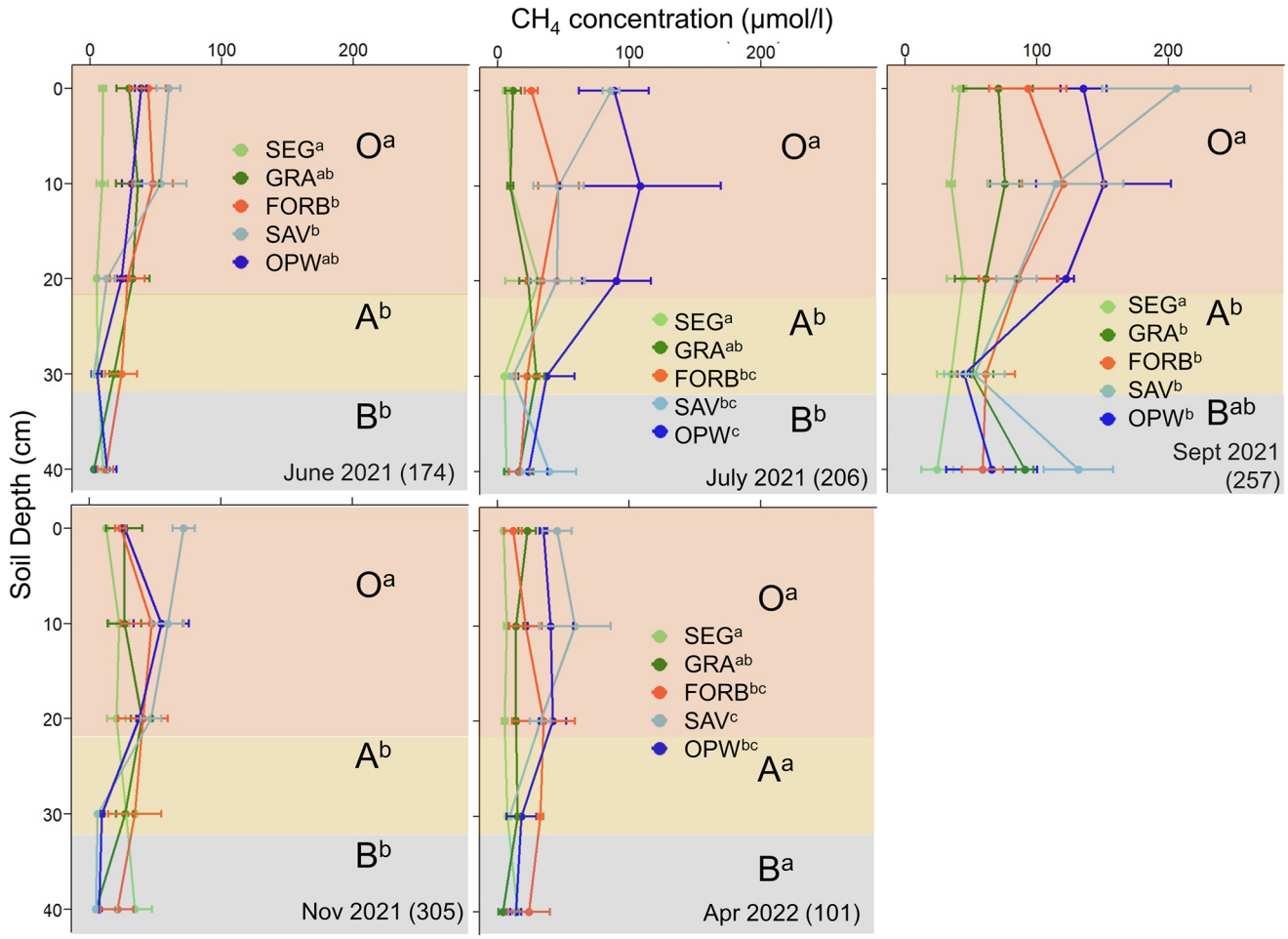

Figure 3. Dissolved porewater CH_4 concentrations (mean ± SE) across soil depth taken during 5 sampling campaigns in 2021/2022 (Julian date). Colored bars indicate approximate soil horizons demarcated in the field (O, A, and B). Letters in superscript indicate significant differences between groups (patch types or soil horizon). SEG = sedges, GRA = grasses, FORB = forbs, SAV = submerged aquatic vegetation, OPW = open water.

3.2. Vegetation Biomass

Aboveground biomass was highest in GRA patches (Table 1) in summer (June, July, and September) but higher in SEG in fall (November) and FORB in spring (April). Belowground biomass was highest in SEG, followed by GRA and FORB, and was several orders of magnitude higher at 0–10 cm depth than 10–40 cm. OPW and SAV had negligible root biomass across all depths.

3.3. Soil Properties

Soil organic carbon (SOC) increased in shallower horizons and was twice as high in O horizons than A and four times higher compared to B horizons (Table S1 in Supporting Information S1). SOC tended to be highest in OPW and lowest in SEG, though differences between patches were not significant. Particle size analysis showed that clay increased with depth similarly across the three patches, from ~12–30%. Soil temperature ranged from 10.0°C to 24.4°C, was cooler with depth and was warmer in OPW and SAV patches compared to emergent vegetation patches (SEG, GRA, and FORB; Figure S5 in Supporting Information S1). Water level was highest in OPW by an average of 26 cm compared to SEG and varied by 30+ cm between its low in July 2021 and high in April 2022 (Table 1; Figure S1 in Supporting Information S1).

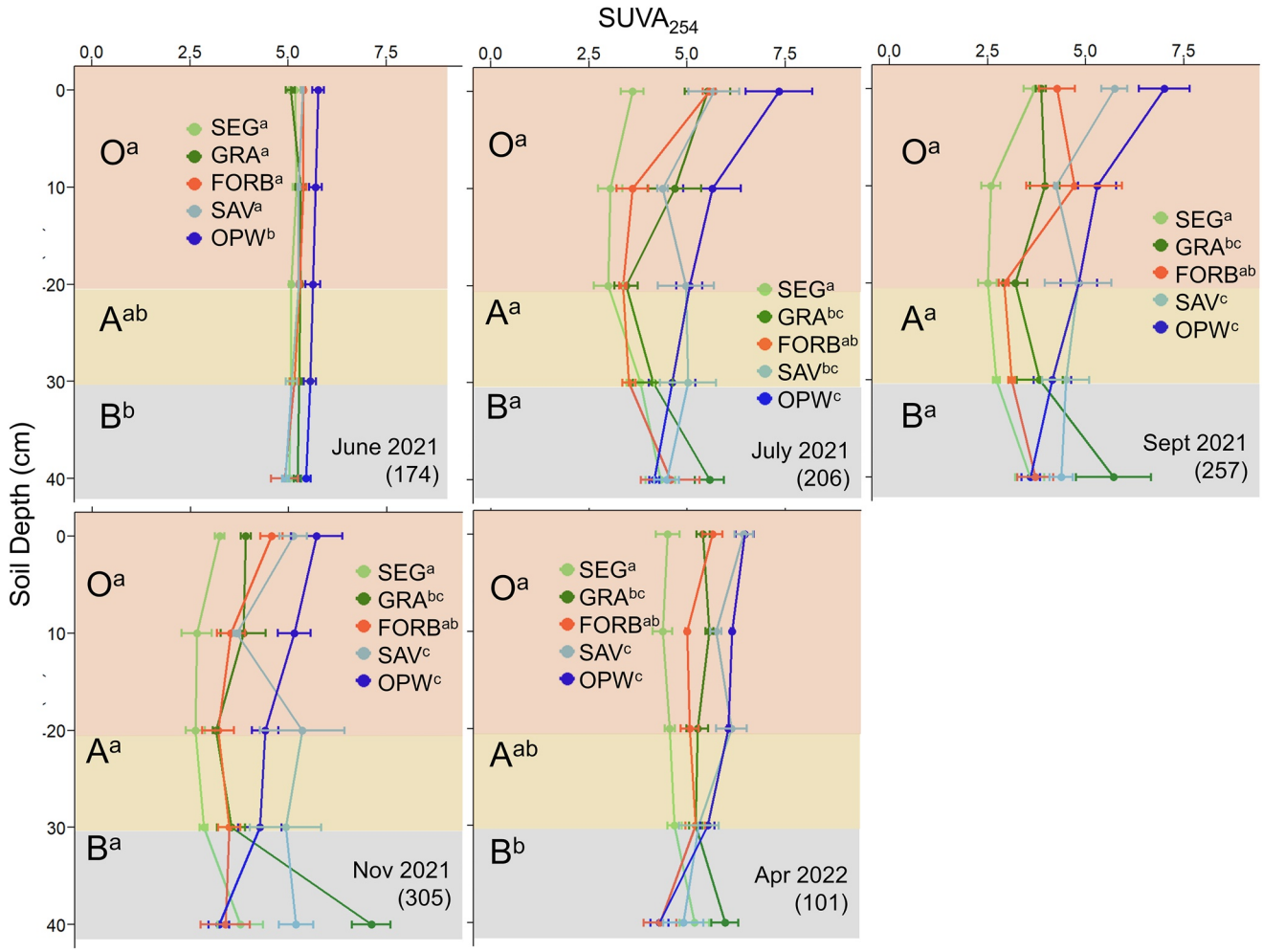

Figure 4. $SUVA_{254}$ values (mean ± SE) across soil depth taken at 5 sampling campaigns in 2021/2022 (Julian date). Higher SUVA values indicate more aromatic or complex dissolved organic carbon. Colored bars indicate approximate soil horizons demarcated in the field (O, A, and B). Letters in superscript indicate significant differences between groups (patch types or soil horizon). SEG = sedges, GRA = grasses, FORB = forbs, SAV = submerged aquatic vegetation, OPW = open water.

3.4. Methane Cycling Microbes

The relative abundance (RA) of methanogens was significantly greater in OPW than GRA (Figure 6). Methanogen RA in FORB patches was similar to GRA in the O horizon, but between GRA and OPW in the A horizon. Methanogen RA in the A horizon exceeded that observed in the O horizon across all patch types.

Methanotrophs followed similar patterns as methanogens: Aerobic methanotrophs were greatest in OPW compared to other patch types and in O compared to A horizons. RA of anaerobic methanotrophs was greater in A horizon and generally increased from GRA to FORB to OPW patches but was not significant (Figure 6).

3.5. Predictors of Porewater Methane

Regression tree analysis and GLMMs both revealed dissolved $[CO_2]$ to be the single most important predictor associated with porewater dissolved $[CH_4]$. In our regression tree analysis, $[CO_2]$, time of year, patch type, temperature, soil depth, and [DOC] were all important predictors of $[CH_4]$ under certain conditions (Figure S6 in Supporting Information S1; total tree $R^2 = 0.64$). When porewater $[CO_2]$ and soil temperature were higher, $[CH_4]$ was greatest (excluding SEG patches where later Julian date was more important than temperature). In deeper soil (≥30 cm) with low [DOC] and $[CO_2]$, $[CH_4]$ was lowest.

In the GLMM, we similarly found that $[CO_2]$, patch type, soil depth, soil temperature, and day of year, were important predictors of $[CH_4]$, with the best-fit model (lowest AIC) including all 5 of these variables (Table 2).

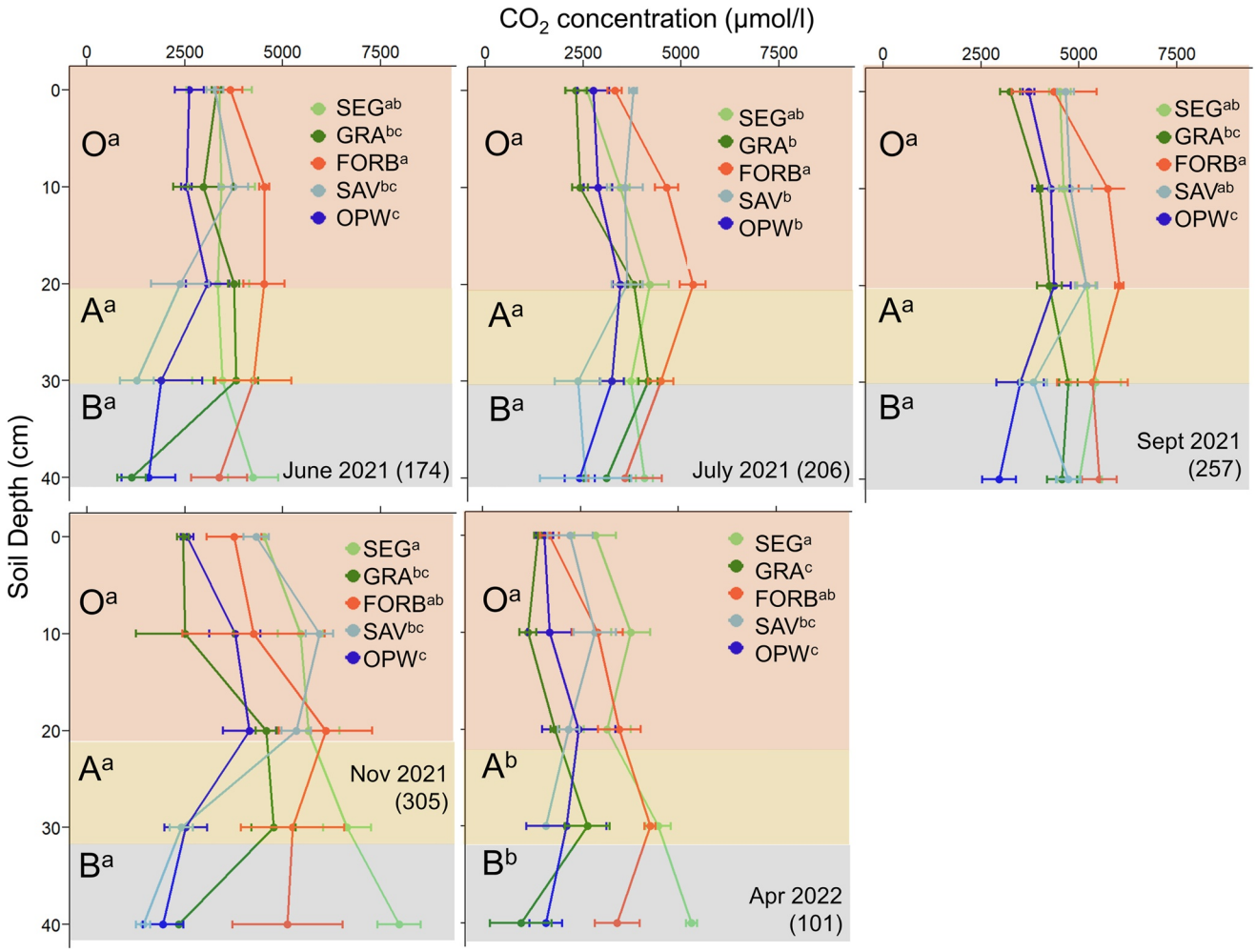

Figure 5. Dissolved porewater CO_2 concentrations (mean ± SE) across soil depth taken at 5 sampling campaigns in 2021/2022 (Julian date). Colored bars indicate approximate soil horizons demarcated in the field (O, A, and B). Letters in superscript indicate significant differences between groups (patch types or soil horizon). SEG = sedges, GRA = grasses, FORB = forbs, SAV = submerged aquatic vegetation, OPW = open water.

Surprisingly, aboveground biomass, microbes, and $SUVA_{254}$ were poor predictors of porewater $[CH_4]$, individually or in combination with other variables. Water level was also a poor predictor of $[CH_4]$, but this was somewhat expected as patches were inundated for most of the study period.

Canopy height of plants explained 50% of the variance in methanogen abundance while $SUVA_{254}$ explained 13% of the variance in aerobic methanotroph abundance (Figure S7 in Supporting Information S1).

3.6. Relative Strength of Predictors

Our structural equation model (SEM) examining the response of porewater dissolved $[CH_4]$ which included patch type, soil depth, $SUVA_{254}$, and dissolved porewater $[CO_2]$ as predictor variables was the best fit of all alternative models (AIC: 7,745, Fisher's $C = 3.79$, $P = 0.44$; Figure 7). We found that patch type was a significant predictor of $[CH_4]$ with OPW having the strongest positive correlation to $[CH_4]$. $[CO_2]$ was the strongest single predictor and was positively correlated with $[CH_4]$ while soil depth was negatively correlated with $[CH_4]$. $SUVA_{254}$ had an indirect effect by modulating $[CO_2]$ and as an endogenous variable (i.e., a dependent variable in the model) was modulated by soil depth and patch type. Soil temperature, water level, campaign date, DOC, and plant metrics were included in alternative SEMs but all failed to improve our model fit.

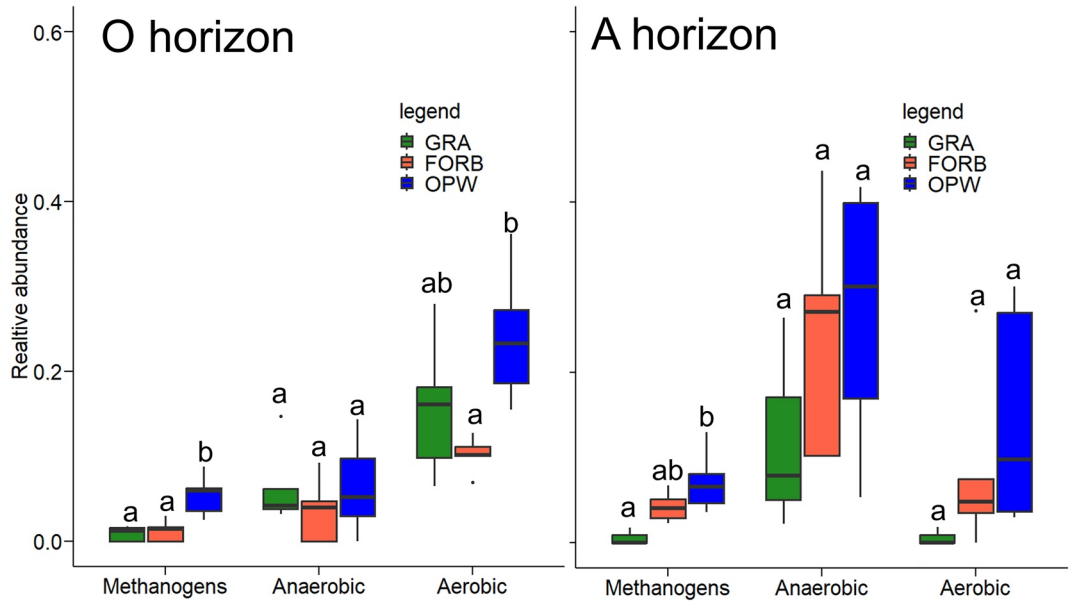

Figure 6. Box plots showing relative abundance of microbes (Methanogens = anaerobic methanogens, Anaerobic = anaerobic methanotrophs, Aerobic = aerobic methanotrophs,) in soil from O and A horizons taken from 3 wetland patches in April and July 2021. Different letters above boxes indicate significant differences between patches. GRA = grasses, FORB = forbs, OPW = open water.

Table 2
Results of Generalized Linear Mixed Models (GLMM) Compared Using AIC Values

Variable ID	Fixed effects	*z*-coeff	R^2_M	R^2_C	AIC	ΔAIC	*P*
Null	~		0	0.14	1,026		
a	Water level	0.2	0.03	0.1	1,019	7	**
b	Patch		0.11	0.15	1,016	10	***
c	CO_2 µmol/l	0.79	0.40	0.70	785	241	***
d	Temp	0.31	0.09	0.20	993	33	***
e	Soil Depth	−0.28	0.07	0.20	1,003	23	***
f	log(AG biomass)	0.06	0.00	0.16	1,028	−2	0.53
g	DOC	0.38	0.12	0.27	982	44	***
h	SUVA	−0.14	0.02	0.19	1,024	2	*
l	Julian date	0.31	0.08	0.21	995	31	***
Mixed models	*b* + *c* + *d* + *e* + *l*		0.68	0.72	645	381	***
	b + *c* + *d* + *e*		0.67	0.71	655	371	***
	c + *d* + *e* + *l*		0.50	0.79	674	352	***
	b + *c* + *d* + *l*		0.59	0.63	740	286	***
	b + *c* + *l*		0.57	0.61	755	271	***
	a+*b* + *c*		0.57	0.61	753	269	***
	a+*c*		0.43	0.68	779	247	***
	c + *g*		0.41	0.69	782	244	***

Note. Multivariate models consist of added individual fixed effects, represented by different letters. Higher ΔAIC indicated better fitting models. R^2_M and R^2_C indicate marginal and conditional R^2 values, respectively. *$P < 0.05$, **$P < 0.01$, ***$P < 0.001$.

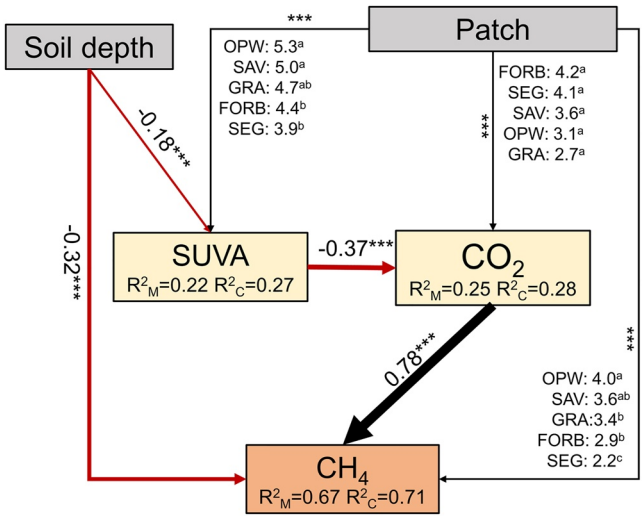

Figure 7. Structural equation model (SEM) showing direct and indirect effects of wetland patch characteristics on the response variable, porewater CH_4 concentrations. Gray boxes indicate exogenous (independent) variables, yellow boxes endogenous (dependent) variables, and orange box the response variable. SUVA represents $SUVA_{254}$ an optical DOC property where higher values indicate more aromatic, plant-like DOC. Arrow size corresponds to z-transformed effect size, labeled above each arrow, with * indicating P-value (***<0.001). Black and red arrows indicate positive and negative relationships, respectively. R^2_M and R^2_C indicate marginal and conditional R^2 values, respectively. The effect of patch, a factorial variable, is shown with marginal means and superscript letters indicate significant difference of effect size between patches (SEG = sedges, GRA = grasses, FORB = forbs, SAV = submerged aquatic vegetation, OPW = open water).

4. Discussion

Porewater dissolved greenhouse gases, including CH_4 and CO_2, represent potential fluxes to the atmosphere and contributors to global warming. Understanding the dynamics of these gases at their source in the soil will help us better understand the connection between CH_4 production, consumption, and flux from the soil or overlying water to the atmosphere. It is documented that plants help predict top-down environmental conditions, including understory community composition and soil properties (Chávez & Macdonald, 2010), while bottom-up environmental filtering can determine plant community assemblages (Lozada-Gobilard et al., 2019). Wetland plants are also known to strongly modulate CH_4 flux to the atmosphere through stomatal conductance, aerenchyma tissue, and root-rhizome architecture (Hirota et al., 2004), but few have studied how plants affect porewater CH_4 or directly measured net in situ CH_4 production in wetland soils. We demonstrate that plant patches, a discrete level of ecological organization in herbaceous wetlands, dominated by common plant functional types (PFT) coalesce many biogeochemical variables either through their co-occurring conditions or through their direct effects on soil properties, uniquely influencing porewater CH_4.

4.1. Patch Differences

We found that herbaceous wetland plant patches do not strongly influence porewater CH_4 concentrations directly (R^2 = 0.11), but patches influence dissolved CO_2, DOC quality, gas transport, and microbial communities to impose significant indirect control on porewater CH_4 (R^2 = 0.68, Table 2, Figure 7). We found that porewater CO_2 concentrations, $[CO_2]$, were the most important variable correlated with porewater $[CH_4]$, perhaps as a terminal electron acceptor in hydrogenotrophic methanogenesis (Figure S8 in Supporting Information S1; Bridgham et al., 2013). Porewater $[CO_2]$ was in turn correlated with DOC quality, specifically $SUVA_{254}$, an indicator of DOC origin and aromaticity. The two graminoid emergent vegetation patches, representing grass and sedge PFTs, corresponded to decreased porewater $[CH_4]$ and shifts in related soil and porewater biogeochemistry, though likely through different mechanisms as discussed below. Microbial relative abundance, although not directly related to $[CH_4]$ in our analysis, also varied among patches and was related to canopy height and DOC quality ($SUVA_{254}$). Patterns of $[CH_4]$ changed over time and with soil depth, with highest $[CH_4]$ in September, when temperatures and water levels were high across the wetland, and in the O horizon where anaerobic methanotrophs were less abundant. This corresponds to other studies of CH_4 emissions from inundated wetlands within our study area, showing high emissions during warm, wet periods suggesting factors controlling CH_4 emissions and production may be related (Hondula, 2021).

Relative elevation and water level likely determine some aspects of soil biogeochemistry at our site via influences on redox conditions that change with the water table (Kottkamp et al., 2022). Likewise, it has been shown that plant patch distributions are driven by hydrology. *Panicum hemitomon* (GRA) can elongate stems in response to increased flooding depth (Kirkman & Sharitz, 1993) while *Carex striata* (SEG) is more tolerant of water drawdown than other species in our study (Laidig, 2012). *Carex* was dominant along the higher edges of the depressional wetland while *Panicum* was found in deeper water less likely of drawdown (Figure 1). *Persicaria hydropiperoides* (FORB), prefers water depth 0–20 cm (Roznere & Titus, 2017), and submerged aquatic vegetation needs a minimum water depth to be erect. However, many variables were better explained by variations in plant physiology and function than water depth.

Dissolved $[CH_4]$ roughly followed a gradient of water depth from lowest in SEG to highest in OPW, though vegetation phenology and physiology affected this relationship. CH_4 produced in the soil must diffuse across the sediment-water interface and through the water column to reach the atmosphere, but plants can bypass this slow diffusion step and emit CH_4 directly to the atmosphere (Bansal et al., 2020; Ström et al., 2003). This could explain the low concentrations of CH_4 we found in patches with emergent vegetation and similarly high

concentrations in OPW and SAV patches under flooded conditions. Soil temperature was consistently lower in emergent patches (SEG, GRA, and FORB), though only by 1–2°C, likely via shading from standing vegetation. However, this subtle difference may lead to a divergence in patch-scale functioning when nonlinear soil temperature thresholds are reached (20°C), particularly those related to the activity of methane cycling microbes (Bansal et al., 2023; Chadburn et al., 2020; Updegraff et al., 1998). Dissolved organic carbon (DOC), the primary substrate for methanogenesis, exhibited seasonal patterns likely related to the PFT in each patch. In SEG, for example, DOC was lowest early in the growing season (April and June) but rapidly increased likely because of root exudation and litter inputs (Uselman et al., 2007).

$[CO_2]$, an important predictor of porewater $[CH_4]$ in our study, was highest in FORB patches and often lowest in OPW, SAV, and GRA patches. Low $[CO_2]$ in OPW and SAV is likely due to low redox potential in deeper water and subsequent decreased rates of soil aerobic respiration (Mitsch & Gosselink, 2000). The low $[CO_2]$ in GRA patches, however, was surprising as these plants are highly productive, can oxygenate the soil through rhizosphere diffusion, and provide ample organic carbon substrate via litter. The accumulation of litter we observed, however, may indicate poor quality and slow decomposition, which is supported by its high litter C:N ratio and decomposition rate compared to other wetland graminoids (Moran et al., 1989). High $[CO_2]$ in FORB patches may also be related to litter quality as similar species have very low C:N (Ren et al., 2022).

$SUVA_{254}$ values strongly differed across patches which also interacted with depth. OPW patches generally decreased with depth, indicating less aromaticity and age (Weishaar et al., 2003) in deeper soil and for the wetlands in our study site, a less plant-like, more microbial-like origin (Hosen et al., 2018). Such a depth related decrease has also been shown in other wetlands in our study site (Wardinski et al., 2022). In emergent patches (SEG and FORB and GRA), we found that $SUVA_{254}$ in shallow porewater was often lower than OPW and SAV patches, suggesting DOC origins here are more microbial-like. However, deeper porewater (B horizon) $SUVA_{254}$ in GRA patches specifically were higher compared to all other patches, suggesting a plant-like origin. This may reflect unique chemical properties of GRA compared to other vegetated patches allowing it to persist in the soil and perhaps demonstrates low palatability for decomposing or methanogenic microbes (Qualls, 2005).

4.2. Links to Methane Dynamics

Our different modeling approaches mostly agreed on the best predictors of observed CH_4 patterns, and particularly on the strong effect of porewater $[CO_2]$, a terminal electron acceptor in hydrogenotrophic methanogenesis. While we did not measure other potential precursors (e.g., acetate), the most abundant methanogen family in our samples was Methanoflorens, which predominantly uses hydrogenotrophic methanogenesis (Figure S8 in Supporting Information S1; Mondav et al., 2014). Furthermore, our SEM suggests that $[CO_2]$ is negatively correlated with $SUVA_{254}$, an indicator of DOC origin and aromaticity. Lower $SUVA_{254}$ values are linked to more microbial than plant-like origins and the correlation of porewater CO_2 and low $SUVA_{254}$ could reflect a greater abundance of CO_2-respiring microbes. Alternatively, as DOC is a substrate for CO_2-respiring decomposers, more aromatic DOC with high $SUVA_{254}$ values may be harder to break down (Qualls, 2005), thus slowing decomposition and the release of $[CO_2]$. Therefore, $SUVA_{254}$ may indirectly control $[CH_4]$ in our soils by modulating the production of the terminal electron acceptor CO_2. This is especially likely in patches dominated by *Panicum hemitomon* (GRA), which produces low quality litter and DOC (Moran et al., 1989).

Soil depth was also a significant predictor according to our models, with $[CH_4]$ generally highest in the O horizon. The greater relative abundance of anaerobic methanotrophs in the A horizon may correspond to more active methanotrophs consuming CH_4 produced under these anoxic conditions. Likewise, fewer anaerobic methanotrophs present in the O horizon may result in a net gain in CH_4 production, causing it to accumulate in this horizon. The resulting reservoirs of CH_4 in the shallow O horizon could be vulnerable to surface disturbance, leading to ebullitive pulses of CH_4 that rapidly bubble to the atmosphere (Sachs et al., 2008).

Patches with dominant PFTs exert unique influences on CH_4 production that can be broadly applied to plant species with similar traits. Both SEG and GRA are functionally similar, large-stature emergent plants yet had very different influences on soil biogeochemistry and CH_4 dynamics. GRA patches produce low quality litter, constraining soil respiration and the production of $[CO_2]$, a key component of hydrogenotrophic methanogenesis (Table 1). SEG patches had low $SUVA_{254,}$ DOC, and high porewater $[CO_2]$ that could support high rates of CH_4 production. Yet *Carex striata* is also known to have highly conductive aerenchyma tissue capable of transporting

oxygen to, and CH_4 from the rhizosphere, suppressing methanogenesis or facilitating atmospheric CH_4 flux, respectively (Visser et al., 2000). *Carex striata* litter also has a low C:N ratios, facilitating high rates of soil respiration, especially when supported by rhizosphere oxygenation (Burrow & Maerz, 2021). Conditions were also ideal for methanogenesis in FORB porewater, which had high porewater [CO_2] and less gas-conductive aboveground biomass compared to graminoid emergent species.

Counter to our model results, OPW had high [CH_4] in July and September despite low [CO_2] and high $SUVA_{254}$ values. We suggest that although rates of CH_4 production may be low due to low [CO_2], CH_4 still accumulates during warmer months by outpacing CH_4 consumption and transport. In unvegetated OPW patches of this study, methanogens are more abundant compared to other patches, soil is more consistently anaerobic, and there is no plant-mediated soil oxygenation to stimulate aerobic oxidation of CH_4. Combined with the lack of plant-mediated gas transport to the surface, the consistent CH_4 production and low rates of consumption and diffusion likely allowed soil CH_4 to accumulate. Previous studies have found similar "reservoirs" of CH_4 in unvegetated soils that were attributed to the lack of plant-mediated fluxes (Bansal et al., 2020; Tokida et al., 2005). SAV patches had the highest [CH_4] in all but July, corresponding with high porewater [CO_2]. Although [DOC] was relatively low and aromatic in SAV, the lack of plant-mediated gas transport and perhaps lateral transport of dissolved CH_4 from nearby sources (e.g., FORB patches) through the soil (something we did not measure) may facilitate accumulation of dissolved CH_4 in shallow soil similar to OPW (Hondula et al., 2021). Although Theus et al. (2023) found fresh plant detritus from SAV, an OM source that may not be well reflected in porewater samples, to be a strong contribution to CH_4 production.

Our analysis of microbial communities suggests a link between porewater [CH_4] and production and consumption rates in the soil, helping to isolate the role of transport in [CH_4] dynamics. Surprisingly, relative abundance of microbes from the three communities we sampled had no relationship with porewater [CH_4]. This could be due to our measure of relative abundance, which tracks the microbial presence rather than activity, and may not reveal differences caused by seasonal shifts in CH_4 production. We also found a negative correlation between canopy cover and methanogen abundance in our study (Figure S4 in Supporting Information S1). This relationship suggests low CH_4 levels in patches like SEG may be due to a lack of production rather than increased transport, as large stature plants like *Carex striata* can deliver significant amounts of oxygen to rhizosphere and soil, inhibiting the establishment of anaerobic methanogen communities (Armstrong et al., 2006). We also observed relatively high levels of SO_4^{2-} in SEG patches, suggesting that oxidizing conditions are prevalent. High oxygen exposure can be lethal to hydrogenotrophic methanogens (Meegoda et al., 2018), the dominant CH_4-producing microbe in our soils. However, as microbial communities are known to vary among species within the same site, we cannot directly infer if the microbial communities between GRA and SEG are similar (Clairmont et al., 2019).

5. Conclusions

Porewater CH_4 represents an important source of atmospheric greenhouse gases and linking it to patch scale drivers can help us understand and predict ecosystem fluxes across herbaceous wetlands. For example, leveraging drivers of CH_4 dynamics (e.g., canopy height, C:N ratio) that are common to patches with a shared PFT allows us to predict patch-scale CH_4 flux without direct measurements now and under future climate scenarios. By mapping PFT distribution in wetlands with field surveys or remote sensing technology we can then aggregate patch-scale estimates of CH_4 to entire wetlands (Cunnick et al., 2023; Niculescu et al., 2020). Although our study was during an unusually wet year, it may foreshadow a typical future year in the mid-Atlantic region of the USA as the climate is predicted to become wetter. Warmer forecasts for the region under future climates could also emphasize the role of shade-providing vegetation as nonlinear temperature thresholds on microbial activity are crossed more frequently or for longer periods (Bansal et al., 2023). Furthermore, shifts in the composition and distribution of vegetation likely to occur with the encroachment of invasive species and changes in climate regimes highlight the need to understand plant influences on soil carbon dynamics. By combining anticipated future vegetation composition in heterogenous herbaceous wetlands with our understanding of how plants mediate CH_4 dynamics, we can greatly improve our accuracy in predicting ecosystem CH_4 fluxes. These estimates can be used to improve global CH_4 budgets or inform conservation and management strategies in herbaceous wetlands to better mitigate greenhouse gas emissions.

Conflict of Interest

The authors declare no conflicts of interest relevant to this study.

Data Availability Statement

Data and code associated with this study are available at the Zenodo open repository at https://doi.org/10.5281/zenodo.10245985 (Sharp et al., 2023).

Acknowledgments
Funding provided by the University of Maryland and NSF DEB# 1856200. We thank the Tully Lab for the use of lab equipment and Chloe Kesey, James Maze, and Alec Armstrong for field assistance. We are also grateful to The Nature Conservancy for permission to access the study sites and stewardship of the land.

References

Armstrong, J., Jones, R. E., & Armstrong, W. (2006). Rhizome phyllosphere oxygenation in Phragmites and other species in relation to redox potential, convective gas flow, submergence and aeration pathways. *New Phytologist*, *172*(4), 719–731. https://doi.org/10.1111/J.1469-8137.2006.01878.X

Bansal, S., Johnson, O. F., Meier, J., & Zhu, X. (2020). Vegetation affects timing and location of wetland methane emissions. *Journal of Geophysical Research: Biogeosciences*, *125*(9), e2020JG005777. https://doi.org/10.1029/2020JG005777

Bansal, S., van der Burg, M., Fern, R. R., Jones, J. W., Lo, R., McKenna, O. P., et al. (2023). Large increases in methane emissions expected from North America's largest wetland complex. *Science Advances*, *9*(9). https://doi.org/10.1126/SCIADV.ADE1112/SUPPL_FILE/SCIADV.ADE1112_SM.PDF

Bates, D., Martin, M., Bolker, B., & Walker, S. (2015). Fitting linear-effects models using lme4. *Journal of Statistical Software*, *67*(1), 1–48. https://doi.org/10.18637/jss.v067.i01

Berberich, M. E., Beaulieu, J. J., Hamilton, T. L., Waldo, S., & Buffam, I. (2020). Spatial variability of sediment methane production and methanogen communities within a eutrophic reservoir: Importance of organic matter source and quantity. *Limnology & Oceanography*, *65*(6), 1336–1358. https://doi.org/10.1002/LNO.11392

Bertness, M. D., & Leonard, G. H. (1997). The role of positive interactions in communities: Lessons from intertidal habitats. *Ecology*, *78*(7), 1976–1989. https://doi.org/10.1890/0012-9658

Boutin, C., & Keddy, P. A. (1993). A functional classification of wetland plants. *Journal of Vegetation Science*, *4*(5), 591–600. https://doi.org/10.2307/3236124

Bridgham, S. D., Cadillo-Quiroz, H., Keller, J. K., & Zhuang, Q. (2013). Methane emissions from wetlands: Biogeochemical, microbial, and modeling perspectives from local to global scales. *Global Change Biology*, *19*(5), 1325–1346. https://doi.org/10.1111/GCB.12131

Burrow, A. K., & Maerz, J. C. (2021). Experimental confirmation of effects of leaf litter type and light on tadpole performance for two priority amphibians. *Ecosphere*, *12*(9), e03729. https://doi.org/10.1002/ECS2.3729

Butterbach-Bahl, K., Papen, H., & Rennenberg, H. (1997). Impact of gas transport through rice cultivars on methane emission from rice paddy fields. *Plant, Cell and Environment*, *20*(9), 1175–1183. https://doi.org/10.1046/J.1365-3040.1997.D01-142.X

Chadburn, S. E., Aalto, T., Aurela, M., Baldocchi, D., Biasi, C., Boike, J., et al. (2020). Modeled microbial dynamics explain the apparent temperature sensitivity of wetland methane emissions. *Global Biogeochemical Cycles*, *34*(11), e2020GB006678. https://doi.org/10.1029/2020GB006678

Chávez, V., & Macdonald, S. E. (2010). The influence of canopy patch mosaics on understory plant community composition in boreal mixedwood forest. *Forest Ecology and Management*, *259*(6), 1067–1075. https://doi.org/10.1016/J.FORECO.2009.12.013

Clairmont, L. K., Stevens, K. J., & Slawson, R. M. (2019). Site-specific differences in microbial community structure and function within the rhizosphere and rhizoplane of wetland plants is plant species dependent. *Rhizosphere*, *9*, 56–68. https://doi.org/10.1016/J.RHISPH.2018.11.006

Cottenie, K. (2005). Integrating environmental and spatial processes in ecological community dynamics. *Ecology Letters*, *8*(11), 1175–1182. https://doi.org/10.1111/J.1461-0248.2005.00820.X

Craft, C. B., Seneca, E. D., & Broome, S. W. (1991). Loss on ignition and kjeldahl digestion for estimating organic carbon and total nitrogen in estuarine marsh soils: Calibration with dry combustion. *Estuaries*, *14*(2), 175–179. https://doi.org/10.1007/BF02689350

Cunnick, H., Ramage, J. M., Magness, D., & Peters, S. C. (2023). Mapping fractional vegetation coverage across wetland classes of sub-Arctic peatlands using combined partial least squares regression and multiple endmember spectral unmixing. *Remote Sensing*, *15*(5), 1440. https://doi.org/10.3390/RS15051440

Donohue, I., Petchey, O. L., Montoya, J. M., Jackson, A. L., Mcnally, L., Viana, M., et al. (2013). On the dimensionality of ecological stability. *Ecology Letters*, *16*(4), 421–429. https://doi.org/10.1111/ELE.12086

Gerard, G., & Chanton, J. (1993). Quantification of methane oxidation in the rhizosphere of emergent aquatic macrophytes: Defining upper limits. *Biogeochemistry*, *23*(2), 79–97. https://doi.org/10.1007/BF00000444/METRICS

Hirota, M., Tang, Y., Hu, Q., Hirata, S., Kato, T., Mo, W., et al. (2004). Methane emissions from different vegetation zones in a Qinghai-Tibetan Plateau wetland. *Soil Biology and Biochemistry*, *36*(5), 737–748. https://doi.org/10.1016/J.SOILBIO.2003.12.009

Hondula, K. L. (2021). *Quantifying effects of seasonal unundation on methane fluxes from forested freshwater wetlands*. University of Maryland.

Hondula, K. L., Jones, C. N., & Palmer, M. A. (2021). Effects of seasonal inundation on methane fluxes from forested freshwater wetlands. *Environmental Research Letters*, *16*(8), 084016. https://doi.org/10.1088/1748-9326/AC1193

Hosen, J. D., Armstrong, A. W., & Palmer, M. A. (2018). Dissolved organic matter variations in coastal plain wetland watersheds: The integrated role of hydrological connectivity, land use, and seasonality. *Hydrological Processes*, *32*(11), 1664–1681. https://doi.org/10.1002/HYP.11519

Inglett, K. S., Inglett, P. W., Reddy, K. R., & Osborne, T. Z. (2012). Temperature sensitivity of greenhouse gas production in wetland soils of different vegetation. *Biogeochemistry*, *108*(1–3), 77–90. https://doi.org/10.1007/S10533-011-9573-3/TABLES/4

Joabsson, A., Christensen, T. R., & Wallén, B. (1999). Vascular plant controls on methane emissions from northern peatforming wetlands. *Trends in Ecology & Evolution*, *14*(10), 385–388. https://doi.org/10.1016/S0169-5347(99)01649-3

Kirkman, L. K., & Sharitz, R. R. (1993). Growth in controlled water regimes of three grasses common in freshwater wetlands of the southeastern USA. *Aquatic Botany*, *44*(4), 345–359. https://doi.org/10.1016/0304-3770(93)90076-9

Kling, G. W., Kipphut, G. W., & Miller, M. C. (1991). Arctic lakes and streams as gas conduits to the atmosphere: Implications for tundra carbon budgets. *Science*, *251*(4991), 298–301. https://doi.org/10.1126/SCIENCE.251.4991.298

Körner, C. (2014). The grand challenges in functional plant ecology. *Frontiers in Plant Science*, *2*, 1. https://doi.org/10.3389/FPLS.2011.00001/BIBTEX

Kottkamp, A. I., Jones, C. N., Palmer, M. A., & Tully, K. L. (2022). Physical protection in aggregates and organo-mineral associations contribute to carbon stabilization at the transition zone of seasonally saturated wetlands. *Wetlands*, *42*(5), 1–17. https://doi.org/10.1007/S13157-022-01557-3

Laidig, K. J. (2012). Simulating the effect of groundwater withdrawals on intermittent-pond vegetation communities. *Ecohydrology*, *5*(6), 841–852. https://doi.org/10.1002/ECO.277

Lefcheck, J. S. (2016). piecewiseSEM: Piecewise structural equation modelling in r for ecology, evolution, and systematics. *Methods in Ecology and Evolution*, *7*(5), 573–579. https://doi.org/10.1111/2041-210X.12512

Lenth, R. (2023). emmeans: Estimated marginal means, aka least-squares means. R package version 1.8.5. Retrieved from https://CRAN.R-project.org/package=emmeans

Lozada-Gobilard, S., Stang, S., Pirhofer-Walzl, K., Kalettka, T., Heinken, T., Schröder, B., et al. (2019). Environmental filtering predicts plant-community trait distribution and diversity: Kettle holes as models of meta-community systems. *Ecology and Evolution*, *9*(4), 1898–1910. https://doi.org/10.1002/ECE3.4883

Meegoda, J. N., Li, B., Patel, K., & Wang, L. B. (2018). A review of the processes, parameters, and optimization of anaerobic digestion. *International Journal of Environmental Research and Public Health*, *15*(10), 2224. https://doi.org/10.3390/IJERPH15102224

Metcalfe, D. B., Fisher, R. A., & Wardle, D. A. (2011). Plant communities as drivers of soil respiration: Pathways, mechanisms, and significance for global change. *Biogeosciences*, *8*(8), 2047–2061. https://doi.org/10.5194/BG-8-2047-2011

Mitsch, W. J., & Gosselink, J. G. (2000). *Wetlands*. Wiley.

Mondav, R., Woodcroft, B. J., Kim, E. H., Mccalley, C. K., Hodgkins, S. B., Crill, P. M., et al. (2014). Discovery of a novel methanogen prevalent in thawing permafrost. *Nature Communications*, *5*(1), 1–7. https://doi.org/10.1038/NCOMMS4212

Moor, H., Rydin, H., Hylander, K., Nilsson, M. B., Lindborg, R., & Norberg, J. (2017). Towards a trait-based ecology of wetland vegetation. *Journal of Ecology*, *105*(6), 1623–1635. https://doi.org/10.1111/1365-2745.12734

Moran, M. A., Hodson, R. E., Fallon, R. D., & Miller, J. D. (1989). Bacterial secondary production on vascular plant detritus: Relationships to detritus composition and degradation rate. *Applied and Environmental Microbiology*, *55*(9), 2178–2189. https://doi.org/10.1128/AEM.55.9.2178-2189.1989

Morrissey, L. A., Zobel, D. B., & Livingston, G. P. (1993). Significance of stomatal control on methane release from *Carex*-dominated wetlands. *Chemosphere*, *26*(1–4), 339–355. https://doi.org/10.1016/0045-6535(93)90430-D

Mueller, P., Mozdzer, T. J., Langley, J. A., Aoki, L. R., Noyce, G. L., & Megonigal, J. P. (2020). Plant species determine tidal wetland methane response to sea level rise. *Nature Communications*, *11*(1), 5154. https://doi.org/10.1038/s41467-020-18763-4

National Research Council. (2001). *Grand challenges in environmental sciences*. The National Academies Press. https://doi.org/10.17226/9975

Niculescu, S., Boissonnat, J. B., Lardeux, C., Roberts, D., Hanganu, J., Billey, A., et al. (2020). Synergy of high-resolution radar and optical images satellite for identification and mapping of wetland macrophytes on the Danube delta. *Remote Sensing*, *12*(14), 2188. https://doi.org/10.3390/RS12142188

Noyce, G. L., & Megonigal, P. J. (2021). Biogeochemical and plant trait mechanisms drive enhanced methane emissions in response to whole-ecosystem warming. *Biogeosciences*, *18*(8), 2449–2463. https://doi.org/10.5194/BG-18-2449-2021

Qualls, R. G. (2005). Biodegradability of fractions of dissolved organic carbon leached from decomposing leaf litter. *Environmental Science and Technology*, *39*(6), 1616–1622. https://doi.org/10.1021/ES049090O/ASSET/IMAGES/LARGE/ES049090OF00003.JPEG

R Core Team. (2019). *R: A language and environment for statistical computing*. R Foundation for Statistical Computing. Retrieved from http://www.r-project.org/

Reddy, K. R., & DeLaune, R. D. (2008). *Biogeochemistry of wetlands: Science and applications*. CRC Press.

Ren, Q., Yuan, J., Wang, J., Liu, X., Ma, S., Zhou, L., et al. (2022). Water level has higher influence on soil organic carbon and microbial community in Poyang Lake wetland than vegetation type. *Microorganisms*, *10*(1), 131. https://doi.org/10.3390/MICROORGANISMS10010131

Roznere, I., & Titus, J. E. (2017). Zonation of emergent freshwater macrophytes: Responses to small-scale variation in water depth1. *Journal of the Torrey Botanical Society*, *144*(3), 254–266. https://doi.org/10.3159/TORREY-D-16-00017.1

Sachs, T., Wille, C., Boike, J., & Kutzbach, L. (2008). Environmental controls on ecosystem-scale CH4 emission from polygonal tundra in the Lena River Delta, Siberia. *Journal of Geophysical Research*, *113*(G3), 0–03. https://doi.org/10.1029/2007JG000505

Saunois, M., Stavert, A. R., Poulter, B., Bousquet, P., Canadell, J. G., Jackson, R. B., et al. (2020). The global methane budget 2000–2017. *Earth System Science Data*, *12*(3), 1561–1623. https://doi.org/10.5194/ESSD-12-1561-2020

Schrier-Uijl, A. P., Kroon, P. S., Hensen, A., Leffelaar, P. A., Berendse, F., & Veenendaal, E. M. (2010). Comparison of chamber and eddy covariance-based CO_2 and CH_4 emission estimates in a heterogeneous grass ecosystem on peat. *Agricultural and Forest Meteorology*, *150*(6), 825–831. https://doi.org/10.1016/J.AGRFORMET.2009.11.007

Sharp, S. J., Maietta, C. E., Stewart, G. A., Taylor, A. K., Williams, M. R., & Palmer, M. A. (2023). Net methane production predicted by patch characteristics in a freshwater wetland (version 2) [Dataset]. Zenodo. https://doi.org/10.5281/zenodo.10245985

Silvey, C., Jarecke, K. M., Hopfensperger, K., Loecke, T. D., & Burgin, A. J. (2019). Plant species and hydrology as controls on constructed wetland methane fluxes. *Soil Science Society of America Journal*, *83*(3), 848–855. https://doi.org/10.2136/SSSAJ2018.11.0421

Ström, L., Ekberg, A., Mastepanov, M., & Christensen, T. R. (2003). The effect of vascular plants on carbon turnover and methane emissions from a tundra wetland. *Global Change Biology*, *9*(8), 1185–1192. https://doi.org/10.1046/j.1365-2486.2003.00655.x

Therneau, T., & Atkinson, B. (2017). rpart: Recursive partioning and regression trees. R package version 4.1.19. Retrieved from https://cran.r-project.org/package=rpart

Theus, M. E., Ray, N. E., Bansal, S., & Holgerson, M. A. (2023). Submersed macrophyte density regulates aquatic greenhouse gas emissions. *Journal of Geophysical Research: Biogeosciences*, *128*(10), e2023JG007758. https://doi.org/10.1029/2023JG007758

Tokida, T., Miyazaki, T., Mizoguchi, M., & Seki, K. (2005). In situ accumulation of methane bubbles in a natural wetland soil. *European Journal of Soil Science*, *56*(3), 389–396. https://doi.org/10.1111/J.1365-2389.2004.00674.X

Updegraff, K., Bridgham, S. D., Pastor, J., & Weishampel, P. (1998). Hysteresis in the temperature response of carbon dioxide and methane production in peat soils. *Biogeochemistry*, *43*(3), 253–272. https://doi.org/10.1023/A:1006097808262/METRICS

Uselman, S. M., Qualls, R. G., & Lilienfein, J. (2007). Contribution of root vs. leaf litter to dissolved organic carbon leaching through soil. *Soil Science Society of America Journal*, *71*(5), 1555–1563. https://doi.org/10.2136/SSSAJ2006.0386

Valentine, D. W., Holland, E. A., & Schimel, D. S. (1994). Ecosystem and physiological controls over methane production in northern wetlands. *Journal of Geophysical Research*, *99*(D1), 1563–1571. https://doi.org/10.1029/93JD00391

Visser, E. J. W., Bogemann, G. M., Van de Steeg, H. M., Pierik, R., & Blom, C. W. P. M. (2000). Flooding tolerance of *Carex* species in relation to field distribution and aerenchyma formation. *New Phytologist*, *148*(1), 93–103. https://doi.org/10.1046/J.1469-8137.2000.00742.X

Von Fischer, J. C., Rhew, R. C., Ames, G. M., Fosdick, B. K., & Von Fischer, P. E. (2010). Vegetation height and other controls of spatial variability in methane emissions from the Arctic coastal tundra at Barrow, Alaska. *Journal of Geophysical Research*, *115*(G4), 0–03. https://doi.org/10.1029/2009JG001283

Waldo, N. B., Hunt, B. K., Fadely, E. C., Moran, J. J., & Neumann, R. B. (2019). Plant root exudates increase methane emissions through direct and indirect pathways. *Biogeochemistry*, *145*(1–2), 213–234. https://doi.org/10.1007/S10533-019-00600-6/FIGURES/7

Wardinski, K. M., Hotchkiss, E. R., Jones, C. N., McLaughlin, D. L., Strahm, B. D., & Scott, D. T. (2022). Water-soluble organic matter from soils at the terrestrial-aquatic interface in wetland-dominated landscapes. *Journal of Geophysical Research: Biogeosciences*, *127*(9), e2022JG006994. https://doi.org/10.1029/2022JG006994

Weiher, E., & Keddy, P. A. (1995). The assembly of experimental wetland plant communities. *Oikos*, *73*(3), 323. https://doi.org/10.2307/3545956

Weishaar, J. L., Aiken, G. R., Bergamaschi, B. A., Fram, M. S., Fujii, R., & Mopper, K. (2003). Evaluation of specific ultraviolet absorbance as an indicator of the chemical composition and reactivity of dissolved organic carbon. *Environmental Science and Technology*, *37*(20), 4702–4708. https://doi.org/10.1021/ES030360X/ASSET/IMAGES/LARGE/ES030360XF00005.JPEG

Wiessner, A., Rahman, K. Z., Kuschk, P., Kästner, M., & Jechorek, M. (2010). Dynamics of sulphur compounds in horizontal sub-surface flow laboratory-scale constructed wetlands treating artificial sewage. *Water Research*, *44*(20), 6175–6185. https://doi.org/10.1016/J.WATRES.2010.07.044

Wilson, J. B., & Agnew, A. D. Q. (1992). Positive-feedback switches in plant communities. *Advances in Ecological Research*, *23*(C), 263–336. https://doi.org/10.1016/S0065-2504(08)60149-X

Woodward, F. I., & Cramer, W. (1996). Plant functional types and climatic changes: Introduction. *Journal of Vegetation Science*, *7*(3), 306–308. https://doi.org/10.1111/J.1654-1103.1996.TB00489.X

References From the Supporting Information

Cawley, K. (2020). *NEON dissolved gas repo*. Github. Retrieved from https://github.com/NEONScience/NEON-dissolved-gas/blob/master/README.md

Helms, J. R., Stubbins, A., Ritchie, J. D., Minor, E. C., Kieber, D. J., & Mopper, K. (2008). Absorption spectral slopes and slope ratios as indicators of molecular weight, source, and photobleaching of chromophoric dissolved organic matter. *Limnology & Oceanography*, *53*(3), 955–969. https://doi.org/10.4319/LO.2008.53.3.0955

Kellerman, A. M., Guillemette, F., Podgorski, D. C., Aiken, G. R., Butler, K. D., & Spencer, R. G. M. (2018). Unifying concepts linking dissolved organic matter composition to persistence in aquatic ecosystems. *Environmental Science and Technology*, *52*(5), 2538–2548. https://doi.org/10.1021/ACS.EST.7B05513/ASSET/IMAGES/LARGE/ES-2017-05513E_0004.JPEG

Li, P., & Hur, J. (2017). Utilization of UV-Vis spectroscopy and related data analyses for dissolved organic matter (DOM) studies: A review. *Critical Reviews in Environmental Science and Technology*, *47*(3), 131–154. https://doi.org/10.1080/10643389.2017.1309186/SUPPL_FILE/BEST_A_1309186_SM2249.DOCX

Viollier, E., Inglett, P. W., Hunter, K., Roychoudhury, A. N., & van Cappellen, P. (2000). The ferrozine method revisited: Fe(II)/Fe(III) determination in natural waters. *Applied Geochemistry*, *15*(6), 785–790. https://doi.org/10.1016/S0883-2927(99)00097-9